Nexo Revista Científica
Vol. 34, No. 03 (Especial), pp. 58-70/Junio 2021

ISSN-E 1995-9516
Universidad Nacional de Ingeniería

https://revistas.uni.edu.ni/index.php/Nexo
https://doi.org/10.5377/nexo.v34i03.11863

Simulation of a continuous fluidised bed dryer for shelled corn†

Simulación de un secador continuo de lecho fluidizado para maíz desgranado

Juan Alonso and Apolinar Picado*

Facultad de Ingeniería Química, Universidad Nacional de Ingeniería (UNI)
Avenida Universitaria, Managua 11127, Nicaragua
E-mail: picado@kth.se

(recibido/received: 12-July-2019; aceptado/accepted: 22-November-2019)

ABSTRACT

In this study, a mathematical model to simulate the drying of shelled corn in a continuous plug-flow fluidised bed dryer is presented. Equipment and material models were applied to describe the process. The equipment model was based on the differential equations obtained by applying mass and energy balances to each element of the dryer. In the case of the material model, mass and heat transfer rates in a single isolated particle were considered. Calculation results were verified by comparison with experimental data from the literature. There was a very good agreement between experimental data and simulation. The effects of gas temperature and velocity, particle diameter, dry solid flow and solid temperature on the drying process were investigated. It was found that the changes in gas velocity, dry solids flow and the solid temperature had essentially no effect on the drying process.

Keywords: Fluidised bed dryer; Plug-flow; Modelling; Shelled corn

RESUMEN

En este estudio, se presenta un modelo matemático para simular el secado de maíz desgranado en un secador continuo de lecho fluidizado con flujo pistón. Se aplicaron modelos para el equipo y del material para describir el proceso. El modelo del equipo se basó en las ecuaciones diferenciales obtenidas al aplicar balances de masa y energía a cada elemento del secador. En el caso del modelo del material, se consideraron las velocidades de transferencia de masa y calor en una sola partícula aislada. Los cálculos se verificaron por comparación con datos experimentales de la literatura. Hubo un muy buen ajuste entre los datos experimentales y la simulación. Se investigaron los efectos de la temperatura y velocidad del gas, el diámetro de las partículas, el flujo de sólidos secos y la temperatura del sólido en el proceso de secado. Se encontró que los cambios en la velocidad del gas, el flujo de sólidos secos y la temperatura del sólido no tuvieron ningún efecto en el proceso de secado.

Palabra claves: Secador de lecho fluidizado; Flujo pistón; Modelación; Maíz desgranado

† Dedicated to Prof. em. Dr.-Ing. habil. Joaquín Martínez on the occasion of his 71st birthday.

* Author for correspondence

1. INTRODUCTION

Corn or maize (*Zea mays* L.) is one of the most widely cultivated grains in the world, which provides a source of high-quality proteins for both feed and food applications. Moisture content is one of the most important factors influencing the quality of corn during storage and it remains at a high level during the harvest of 32-43% (dry basis). Drying is the most widely practised preservation method for shelled corn. The moisture content of shelled corn is lowered during drying to the level of 16-17% (dry basis) at which there is no danger of the growth of undesirable microorganisms (Sun, 1998; Abdoli *et al*., 2018).

Fluidised bed drying is the most commonly used drying method to preserve foods and agricultural products and among several methods for drying moist granular materials, fluidised bed drying has been one of the most successful techniques and widely used during postharvest processing of agricultural grain (Mujumdar, 2014). In this drying method, solid moist particles are suspended in a hot air stream and a high rate of heat and mass transfer takes place between the grain and gas.

Numerous types of fluidised bed dryers have been developed in various industries, among which, well-mixed, plug-flow, vibrated, agitated and centrifugal fluidised bed dryers are the most important ones. Despite this variety, the well-mixed and plug-flow fluidised bed dryers are the most common types, which can cover other above-mentioned types of dryers.

Most of the existing models of plug-flow fluidised bed dryers are based on knowledge of the interaction between the solid and gas phases. For instance, Zoghi *et al*. (2018) developed a model for a cross-flow fluidised bed dryer by considering axial dispersion and expanded it to a three-story dryer (i.e., three sequential single-story dryers). The comparison with experimental results showed that the model can reasonably predict the drying process. Khanali *et al*. (2018) reported a model for a plug-flow fluidised bed dryer. The model was developed by using the mass balance of moisture content inside a control volume of the bed based on the axial dispersion phenomenon. A satisfactory agreement between simulated and experimental results was achieved. Further, Khanali *et al*. (2014) presented a model for a plug-flow fluidised bed dryer under dynamic conditions resulted from the transient of inlet dry solids mass flow rate. The model equations were solved numerically using the finite difference method. Additionally, Khanali *et al*. (2013) reported a model for a plug-flow fluidised bed dryer under steady-state conditions based on partial differential equations. A very satisfactory agreement between the theoretical and experimental data was achieved. Bizmark *et al*. (2010) reported a sequential method to model a continuous plug-flow fluidised bed dryer, which is based on dividing the dryer into sections in series with ideal mixing for both solid and gas phases in each section. It was shown that the model fitted the experimental data satisfactorily. Daud (2007) has used the steady-state cross-flow model for estimating the profiles for solids and air moisture contents and temperatures in a continuous fluidised bed dryer. These profiles were shown to be dependent on the gas-solid flow ratio. Izadifar and Mowla (2003) developed a mathematical model to simulate the drying of moist paddy rice in a cross-flow continuous fluidised bed dryer, applying momentum, mass and energy balances to each element of the dryer. Also, the non-ideal flow of solids in plug-flow fluidised dryers has been modelled as several continuous back-mixed fluidised bed dryers connected in several ways (Wanjari *et al*., 2006; Baker *et al*., 2010). The problem with this type of model is the difficulty of estimating enough completely mixed dryers for any dryer a priori. It could only be determined by an analysis of pilot-plant data (Daud, 2008).

Building on the results of an earlier study (Picado and Martinez, 2012), the present work was aimed to study the mathematical modelling and simulation of a continuous fluidised bed dryer for shelled corn. This was done by incorporating a material model for a single wet grain, amenable to be solved analytically, in an incremental equipment model assuming plug-flow of the solids with gas cross-flow. The validity of the model was tested by comparison of model predictions with experimental data from the literature.

2. DESCRIPTION OF THE MODEL

A schematic description of the continuous plug-flow fluidised bed dryer is shown in Fig. 1. Shelled corn particles enter the dryer by a helical feeder and are fluidised smoothly by the upward flow of gas, normally air coming from the bottom of the bed through a gas distributor. Effective mixing of the shelled corn particles takes place and a homogeneous material at a vertical cross-section of the dryer is usually obtained. Due to fluidisation and the slope of the dryer, shelled corn particles move forward along the dryer and a partially dry product exits from the end.

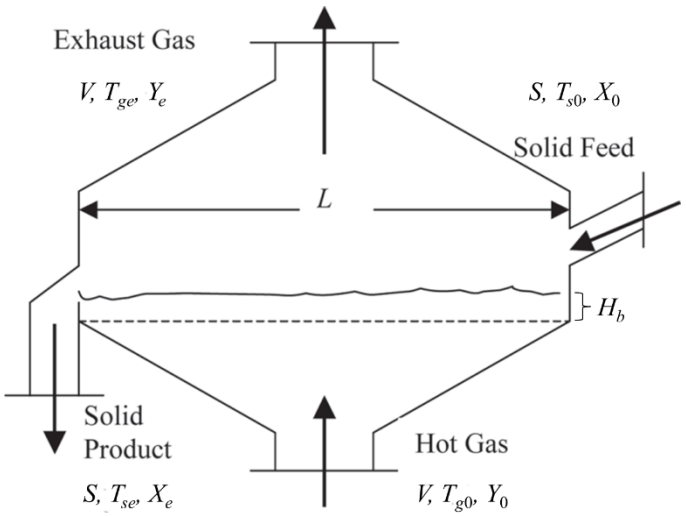

Fig. 1 A plug-flow fluidised bed dryer.

The details of the model have been presented elsewhere (Picado and Martínez, 2012) and only the essentials are outlined here. The following assumptions are introduced to simplify the complex characteristics of the process in the dryer:

- Shelled corn is a spherical grain, isotropic, uniform in size and homogenous.
- The grain is perfectly well mixed in the vertical direction.
- Shrinkage of the grain during drying is negligible.
- Physical properties of the dry grain remain constant with time.
- The inlet distribution of the moisture content and temperature is uniform.
- Heat and mass transfer inside the grain takes place only in the radial direction.
- Moisture at the grain surface is in equilibrium with the gas humidity.
- The dryer is perfectly insulated.

2.1 Mass and energy balances

In the analysis of the dryer, it was assumed that the bed of particles was moving forward at a uniform velocity and that the dryer had been operating for long enough to ensure that steady-state conditions were reached. A moisture balance applied to the differential volume element shown in Fig. 2 yields:

$$F_s \frac{dX_b}{dz} = - a_s M G_g \tag{1}$$

where X is the solid moisture content on a dry basis, M is the molecular weight of the moisture, a_s is the specific evaporation area per unit bed volume, G_g is the molar evaporation flux, F is a mass flow per cross-section in the direction of the flow, and z is the distance along the bed from the solids inlet. The subscripts s and b denote solid and bed, respectively.

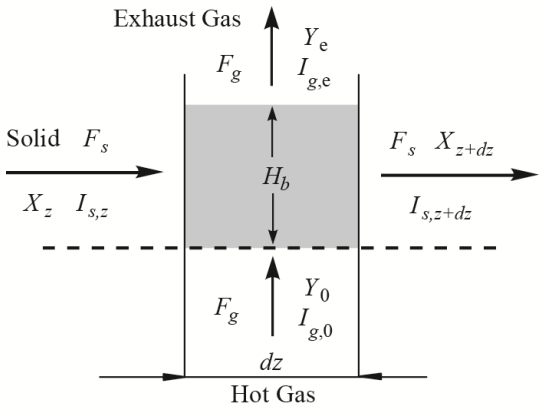

Fig. 2 Scheme of a differential dryer element.

Because all of the evaporated liquid goes to the gas, the following equation gives the change in gas humidity:

$$F_g\, dY = -F_s\, H_b \frac{dX_b}{dz} \tag{2}$$

where Y is the gas humidity on a dry basis and H_b is the bed height. The subscript g denotes gas. The bed height is calculated as

$$H_b = \frac{S}{v\rho_p(1-\varepsilon_p)(1-\varepsilon_b)B} \tag{3}$$

where S is the flow of dry solids, v is forward bed velocity, ρ is the density, ε is the porosity, and B is the dryer width. The subscript p denotes particle. Because heat losses in the dryer are neglected, the energy balance over the same differential volume element becomes

$$dI_g = -H_b \frac{F_s}{F_g} \frac{dI_s}{dz} \tag{4}$$

where I is the enthalpy of the phases per unit mass on a dry basis. To integrate Eq. (1) to determine the changes in mean moisture content of the grain along the dryer, in addition inlet conditions, the evaporation flux must be provided. This flux depends on the temperature and moisture content at the surface of the particles. This information can be obtained by analysing what happens with a single particle moving along the dryer.

2.2 Drying of a single particle

The drying of a single wet particle into an inert gas is schematically described in Fig. 3. During the drying process, the moisture migrates from the centre of the solid particle towards the surface, where it

evaporates. Migration occurs due to the moisture gradient in the solid particle by several mechanisms: molecular diffusion (liquid and vapour), capillary flow, Knudsen diffusion, surface diffusion, or combinations of the foregoing mechanisms. Usually, all of these mechanisms are lumped into an effective liquid transport mechanism using Fick's law for mass flux, which seems to describe the experimental data fairly well (Mujumdar, 2014; Saravacos and Maroulis, 2001).

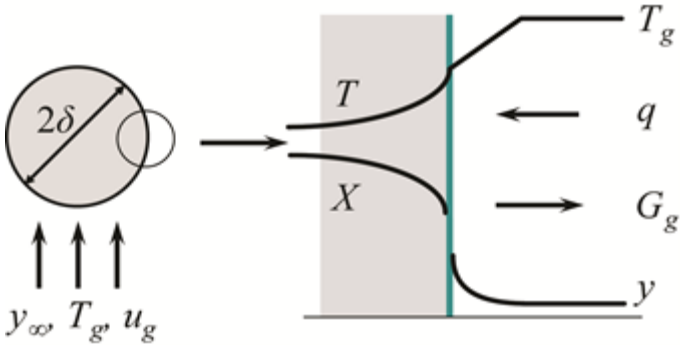

Fig. 3 Schematic of drying of a single particle into a gas.

Based on the assumptions outlined above, a set of space-averaged governing equations can be written for the particle. The longitudinal location of a particle in the dryer is related to the residence time (t) by the linear velocity of the bed (v). This allows one to track the changes in moisture content and temperature of particles as functions of distance along the bed (z). By introducing this change in variables, the diffusion equation for the spherical particle is

$$v\frac{\partial X}{\partial z} = D_{eff}\left(\frac{\partial^2 X}{\partial r^2} + \frac{2}{r}\frac{\partial X}{\partial r}\right) \tag{5}$$

where r is the radial coordinate and D_{eff} is the effective diffusion coefficient, which is estimated using an equation reported by Chu and Hustrulid (1968).

If conduction is the only mechanism for heat transfer within the particle, the corresponding equation to describe temperature changes is the conduction equation:

$$v\frac{\partial T}{\partial z} = D_h\left(\frac{\partial^2 T}{\partial r^2} + \frac{2}{r}\frac{\partial T}{\partial r}\right) \tag{6}$$

where D_h is the thermal diffusivity of the wet grain and T is the temperature. Equations (5) and (6) represent a system of partial differential equations with the following inlet and boundary conditions:

At $z = 0$ and $0 \le r \le \delta$,

$$X = X_0\{r\}; \qquad T = T_0\{r\} \tag{7}$$

At $z > 0$ and $r = 0$,

$$\frac{\partial X}{\partial r} = 0; \qquad \frac{\partial T}{\partial r} = 0 \tag{8}$$

At $z > 0$ and $r = \delta$,

$$-\rho_p D_{eff} \frac{\partial X}{\partial r} = M G_g ; \quad -k_{eff} \frac{\partial T}{\partial r} = h(T - T_{g,\infty}) + \lambda G_g \tag{9}$$

where δ is the particle radius, k is the thermal conductivity of the wet solid, and λ is the latent heat of vaporisation. The subscripts 0, *eff*, and ∞ denote inlet, effective value, and gas bulk, respectively. Effective physical properties can be estimated by averaging the corresponding properties of the solid and moisture.

2.3 Mass and Heat Transfer Rates

At the interphase, the evaporation flux is simply calculated as

$$G_g = k_m (y_\delta - y_\infty) \tag{10}$$

where k_m is the mass transfer coefficient, and y_δ and y_∞ are the vapour molar fractions at the gas-wet solid interface and in the gas bulk, respectively. In a hygroscopic material, the vapour pressure at the surface will be lower than the saturated value. This is accounted for by introducing a sorption isotherm that relates the equilibrium vapour pressure at the solid surface to the saturated value. In the present study, an empirical equation reported by Pfost *et al*. (1976) is used to correlate experimental equilibrium data. This information is inserted into Eq. (10), where y_δ is given by the ratio between the partial pressure of water vapour and the total pressure.

The convective heat flux can be calculated as:

$$q = h (T_{g,\infty} - T_\delta) \tag{11}$$

where h is the heat transfer coefficient between the drying gas and particle and is estimated using a correlation reported by Yang (2003). The mass transfer coefficient can be calculated from the heat transfer coefficient by applying the Lewis relationship because the Prandlt and Schmidt numbers are almost equal for mixtures of water vapour and air (Mujumdar, 2014).

2.4 Implementation of the model

Equation (1) is a nonlinear ordinary differential equation that can be solved numerically using Euler's or any other standard method. Mass and heat transfer rates are required in the mass and energy balances along the dryer. The simultaneous solution of Eqs. (5) and (6), subjected to inlet and boundary conditions (7) through (9), provides the moisture content and temperature gradients in the particle as well as mass and heat transfer rates at the particle surface. By assuming constant transport coefficients as well as constant mass and heat transfer rates in each integration step of Eq. (1), Eqs. (5) and (6) can be solved analytically. The details of the analytical solutions and dimensionless variables as well as other parameters of the solutions can be found elsewhere (Picado and Martínez, 2012).

Because the conditions change along the dryer, the analytical solutions are applied to an interval dz, with inlet conditions and averaged transport coefficients corresponding to the outlet conditions of the previous step. As the integration of Eq. (1) proceeds, the procedure is repeated step by step. The outlet composition of the gas at each step dz is calculated using Eq. (2). Then the energy balance, Eq. (4), allows for the calculation of the exhaust gas enthalpy using the mean particle temperature to calculate the outlet enthalpy of the wet solids. Because the gas enthalpy is a function of gas composition and temperature, the outlet

gas temperature can be calculated from a nonlinear equation that relates gas temperature with the gas enthalpy. Integration proceeds in this way until the dryer exit is reached.

3. RESULTS AND DISCUSSION

3.1 Model validation

To investigate the validity of the model predictions, the theoretical results were compared with pilot-scale experimental data from the literature. The material under consideration was shelled corn (single cross 704 variety) from the Moghan region, Iran. The experimental plug-flow fluidised bed dryer consisted of a chamber with a rectangular cross-section for the gas flow of 1 m × 0.08 m and a height of 0.4 m. To measure the moisture content, sampling was performed at three points along the dryer length at 0.1, 0.5 and 0.9 mm from the solid inlet port. Details of the experimental procedure can be found elsewhere (Khanali *et al*., 2013). The experimental data sets were either cited directly from tables or read (digitised) from experimental points on figures in Khanali *et al*. (2018). The basic physical properties of shelled corn used in the simulation are summarised in Table 1.

Table 1 Physical properties of shelled corn (Khanali *et al*., 2018; Lee and Chung, 1995).

Particle diameter (m)	7.9×10^{-3}
Particle density (kg/m^3)	1185
Particle porosity	0.3755
Specific heat (J/kg K)	1532
Thermal conductivity (W/m K)	0.1405

Figures 4 and 5 show a comparison between the mean moisture content predicted by the mathematical model and experimental data for the same operating conditions. Both cases exhibited a very good agreement with the experimental data. As can be seen in Figs. 4 and 5, the predicted and experimental moisture contents exhibited a smooth exponential decay curve over the whole length of the dryer that characterises the drying in the falling rate period for hygroscopic materials. Air drying of many foods and agricultural products, such as shelled corn, displays no constant rate period and the internal resistance to moisture transfer controls the drying process (Mujumdar, 2014). Further, similar axial profiles of moisture content for plug-flow fluidised bed drying employing different materials have been reported (Baker *et al*., 2006; Wanjari *et al*., 2006; Baker *et al*., 2010; Janas *et al*., 2010; Khanali *et al*., 2013).

Unlike previous models, the mathematical model does not require to include the axial dispersion for accurately modelling the drying process, and therefore modelling the discontinuity at the solid inlet port of the dryer due to the axially dispersed flow of solid particles inside the bed and the plug-flow of the feed particles at the solid inlet port reported by Khanali *et al*. (2018). Moreover, the dispersion coefficient is not a very accurate measurable parameter. It is highly dependent on dryer configuration (bed geometry), material properties, and operating conditions (Nilsson, 1986).

Furthermore, Baker *et al*. (2006) reported the unexpected result that dispersion had essentially no effect on the moisture content and temperature profiles. They also suggested that the effects of dispersion might be more pronounced in the case of non-hygroscopic materials. Later, Baker *et al*. (2010) proved the hypothesis and found that the effect of dispersion on the moisture profile was more pronounced for the non-hygroscopic material than for the hygroscopic material. It was concluded that, under normal operating conditions, the effect of dispersion on the performance of plug-flow fluidised bed dryers can be neglected under all circumstances. It would be desirable to confirm this experimentally, however.

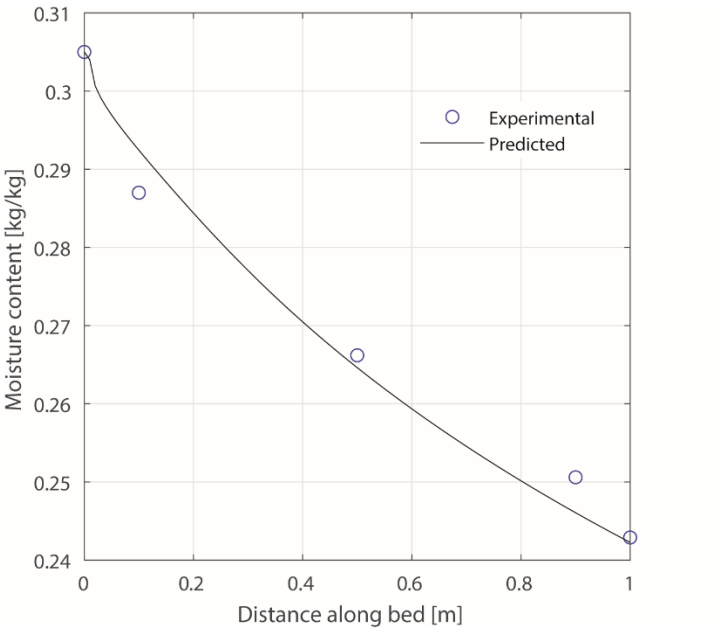

Fig. 4 Comparison between experimental and predicted moisture content along the bed length. u_g = 3 m/s, $T_{g,0}$ = 343.15 K, Y_0 = 0.0010 kg/kg, S = 0.0094 kg/h, X_0 = 0.305 kg/kg, $T_{s,0}$ = 301.15 K, v = 0.008 m/s.

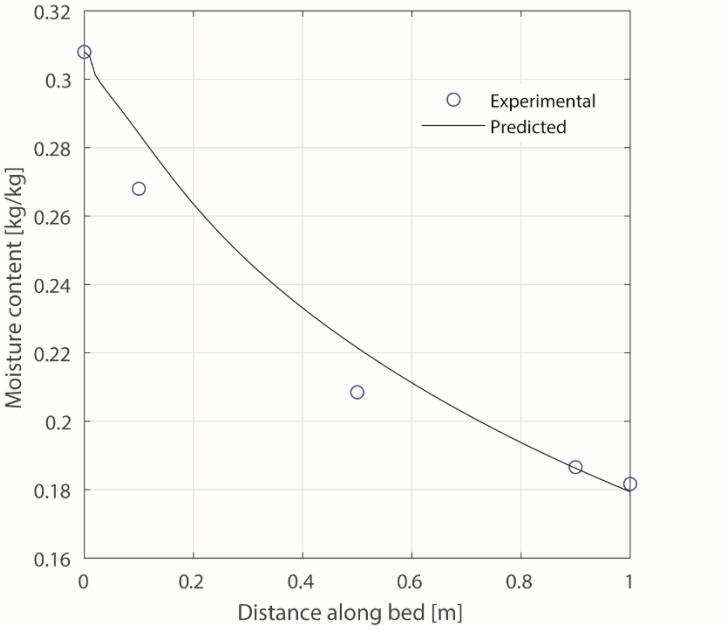

Fig. 5 Comparison between experimental and predicted moisture content along the bed length. u_g = 3 m/s, $T_{g,0}$ = 373.15 K, Y_0 = 0.0018 kg/kg, S = 0.0041 kg/h, X_0 = 0.308 kg/kg, $T_{s,0}$ = 301.15 K, v = 0.005 m/s.

In a plug-flow fluidised bed dryer, the temperature of the solids progressively rises as they move from the feed point to the dyer exit. However, in this case, the predicted solid temperature increases rapidly within a short distance from the solid inlet port (results not shown) and approaches a temperature nearly the same as the drying air temperature, and then remains nearly constant until the dryer exit. Khanali *et al*. (2013) reported a similar experimentally behaviour for rough rice drying in a plug-flow fluidised bed dryer and then confirmed by Picado and Gamero (2014) employing simulations.

A parity plot of the measured and predicted values of mean solid moisture content for both continuous plug-flow fluidised bed drying experiments are shown in Fig. 6. The predicted and measured values agree very well for both drying experiments. The data points are banded around a 45° straight line, thereby demonstrating the suitability of the model in predicting the variation of the moisture content. Therefore, the present model correctly describes the drying process with good accuracy.

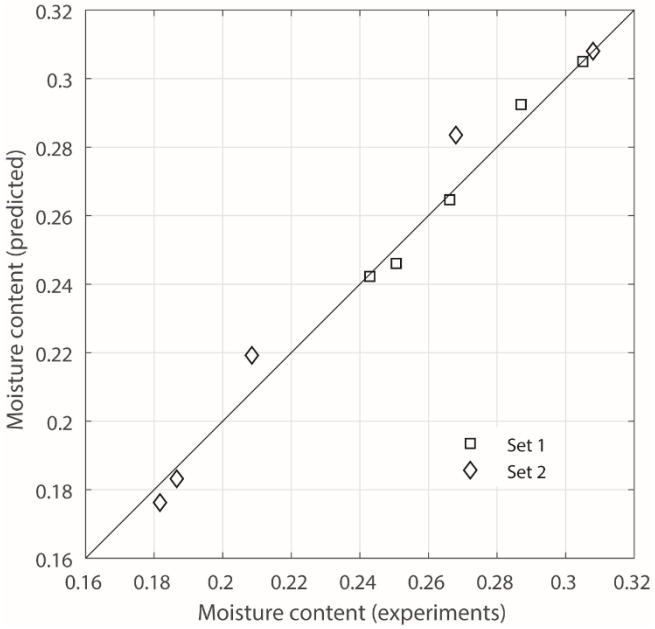

Fig. 6 Comparison of predicted and experimental values of solid moisture content.

3.2 Parametric studies

Because knowledge of the parameters that significantly impact drying behaviour is useful in designing dryers, simulations were extended to predict the effects of operating parameters. The basic data used in the simulations that follow were the same as those in Fig. 4. In all cases, a ± 15% variation in the operating parameters was applied.

Effect of inlet gas temperature

Figure 7 depicts the effect of inlet gas temperature (60 to 80ºC) on the moisture content profile along the length of the dryer. As expected, the evaporation (drying) rate increases with the inlet gas temperature, thus resulting in lowering solid moisture content. This effect can be attributed to the controlling rate of water vapour transfer inside the grain due to moisture diffusion towards the surface. Further, the solid temperature increases with an increase in the inlet gas temperature.

Effect of particle size

Figure 8 illustrates the effect of particle diameter on the moisture content profile along the length of the dryer. As shown in Fig. 8, increasing the particle diameter reduces the evaporation of the solid moisture content. Larger particles contain much longer diffusional paths within the solid, thus increasing internal resistance against mass transfer. The changes in particle diameter had very little effect on the solid temperature along the length of the dryer (results not shown).

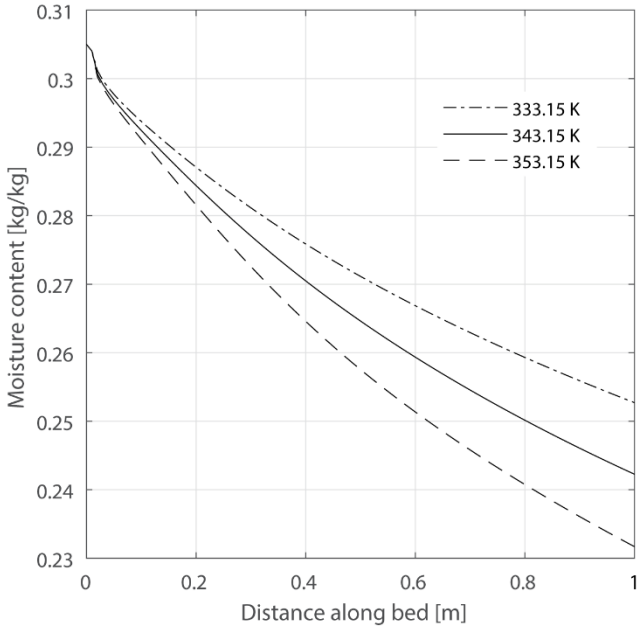

Fig. 7 Effect of gas temperature on drying behaviour. u_g = 3 m/s, Y_0 = 0.0010 kg/kg, S = 0.0094 kg/h, X_0 = 0.305 kg/kg, $T_{s,0}$ = 301.15 K, v = 0.008 m/s.

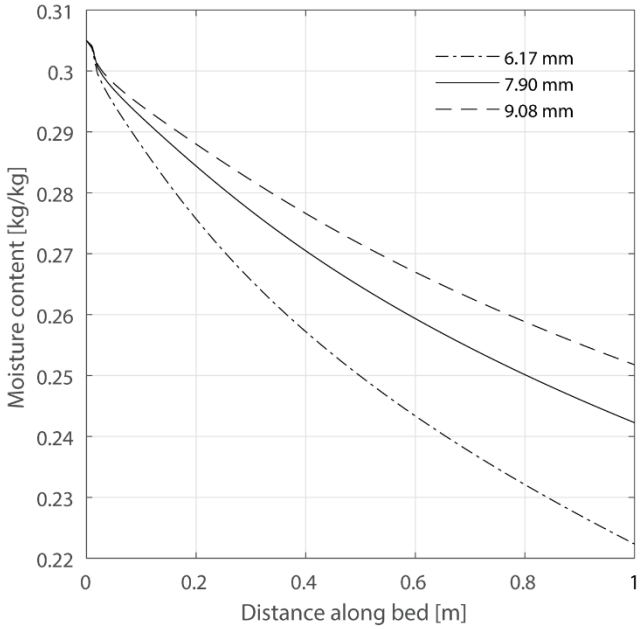

Fig. 7 Effect of particle size on drying behaviour. u_g = 3 m/s, $T_{g,0}$ = 343.15 K, Y_0 = 0.0010 kg/kg, S = 0.0094 kg/h, X_0 = 0.305 kg/kg, $T_{s,0}$ = 301.15 K, v = 0.008 m/s.

At the conditions chosen for calculations, it was found that changes in gas velocity, dry solid flow, and the solid temperature had essentially no effect on drying behaviour. A similar result has also been reported by Bizmark *et al*. (2010) and Khanali *et al*. (2013).

The solid moisture contents decrease non-linearly along the length of the dryer as shown in Figs. 6 and 7. Similar results were reported by Khanali *et al*. (2013), Picado and Martínez (2012) and Nilsson (1986) for

rough rice, corn grits and apatite granules, respectively. However, a linear decreasing moisture content profile along the length of a continuous plug-flow fluidised bed dryer was also reported in the literature (Izadifar and Mowla, 2003).

4. CONCLUSIONS

In this study, a continuous plug-flow fluidised bed dryer model has been presented and validated. The predicted moisture content using the proposed model showed a very good agreement with experimental data. Simulations based on this model were conducted to study the effects of operating parameters, such as gas temperature, gas velocity, particle size, dry solids flow and inlet solid temperature on the moisture content. An increase in gas temperature induces faster drying. As the particle diameter was increased, the drying process slowed down. In these calculations, gas velocity, dry solids flow, and the solid temperature had essentially no effect on the drying process. The present model could be a useful tool for process exploration and optimisation of this type of dryer.

CONFLICT OF INTERESTS

The authors declare that there is no conflict of interests regarding the publication of this article.

ACKNOWLEDGEMENTS

The authors gratefully acknowledge the partial financial support provided by the Swedish International Development Cooperation Agency (Sida). A. Picado also acknowledges Panabits, Panama for providing the digitalisation of the experimental data.

NOTATION

a_s	Specific area per unit bed volume	(m^2 m^{-3})
B	Dryer width	(m)
D	Mass transport coefficient	(m^2 s^{-1})
D_h	Thermal diffusivity	(m^2 s^{-1})
F	Mass flow per cross-section, dry basis	(kg m^{-2} s^{-1})
G_g	Molar evaporation flux	(kmol m^{-2} s^{-1})
h	Heat transfer coefficient	(W m^{-2} K^{-1})
H_b	Bed height	(m)
I	Enthalpy per unit mass, dry basis	(J kg^{-1})
k	Thermal conductivity	(W m^{-1} K^{-1})
L	Dryer length	(m)
M	Molecular weight of the moisture	(kg $kmol^{-1}$)
q	Heat flux	(J m^{-2} s^{-1})
r	Radial coordinate	(m)
S	Flow of dry solids	(kg s^{-1})
t	Time	(s)
T	Temperature	(K)
u_g	Gas velocity	(m s^{-1})
V	Flow of dry gas	(kg s^{-1})
v	Forward bed velocity	(m s^{-1})
X	Solid moisture content, dry basis	(kg kg^{-1})
y	Molar fraction in the gas phase	(kmol $kmol^{-1}$)
Y	Gas humidity, dry basis	(kg kg^{-1})
z	Distance along the length of the bed	(m)

Greek Letters

δ	Particle radius	(m)
ε	Porosity	(-)
λ	Latent heat of vaporisation	(J kmol^{-1})
ρ	Density	(kg m^{-3})

Subscripts

b	Bed	*s*	Solid
e	Exit	*t*	Total
eff	Effective value	δ	Interface
g	Gas	∞	Gas bulk
p	Particle	0	Inlet

REFERENCES

Abdoli, B., Zare, D., Jafari, A., & Chen, G. (2018). Evaluation of the air-borne ultrasound on fluidized bed drying of shelled corn: Effectiveness, grain quality, and energy consumption. *Drying Technology*, 36(14), 1749-1766. doi: 10.1080/07373937.2018.1423568

Baker, C.G.J., & Lababidi, H.M.S. (2010). An improved model of plug-flow fluidized bed dryers with an emphasis on energy conservation. *Drying Technology*, 28(5), 730-741. doi: 10.1080/07373931003799368

Bizmark, N., Mostoufi, N., Sotudeh-Gharebagh, R., & Ehsani, H. (2010). Sequential modeling of fluidized bed paddy dryer. *Journal of Food Engineering*, 101(3), 303-308. doi: 10.1016/j.jfoodeng.2010.07.015

Chu, S.T., & Hustrulid, A. (1968). Numerical solution of diffusion equations. *Transactions of the ASAE*, 11(5), 705-0708. doi: 10.13031/2013.39503

Daud, W.R.W. (2008). Fluidized bed dryers-Recent advances. *Advanced Powder Technology*, 19(5), 403-418. doi: 10.1016/S0921-8831(08)60909-7

Daud, W.R.W. (2007). A cross-flow model for continuous plug flow fluidized-bed cross-flow dryers. *Drying Technology*, 25(7-8), 1229-1235. doi: 10.1080/07373930701438618

Izadifar, M., & Mowla, D. (2003). Simulation of a cross-flow continuous fluidized bed dryer for paddy rice. *Journal of Food Engineering*, 58(4), 325-329. doi: 10.1016/S0260-8774(02)00395-3

Khanali, M., Giglou, A.K., & Rafiee, S. (2018). Model development for shelled corn drying in a plug flow fluidized bed dryer. *Engineering in Agriculture, Environment and Food*, 11(1), 1-8. doi: 10.1016/j.eaef.2017.09.002

Khanali, M., Rafiee, S., & Jafari, A. (2014). Numerical simulation and experimental investigation of plug-flow fluidized bed drying under dynamic conditions. *Journal of Food Engineering*, 137, 64-75. doi: 10.1016/j.jfoodeng.2014.03.020

Khanali, M., Rafiee, S., Jafari, A., & Hashemabadi, S.H. (2013). Experimental investigation and modeling of plug-flow fluidized bed drying under steady-state conditions. *Drying Technology*, 31(4), 414-432. doi: 10.1080/07373937.2012.738751

Lee, C.H., & Chung, D.S. (1995). Grain physical and thermal properties related to drying and aeration. In Grain drying in Asia: proceedings of an international conference held at the FAO Regional Office for Asia and the Pacific, Bangkok, Thailand, 17-20 October 1995. Canberra: Australian Centre for International Agricultural Research, 1996.

Mujumdar, A.S. (2014). Handbook of Industrial Drying, 4th ed. CRC Press. Boca Raton, USA. doi: 10.1201/b17208

Nilsson, L. (1986). Behaviour of longitudinal-flow, vibrating fluid-bed dryers. An experimental and theoretical study. PhD Thesis. Lund Univ. Dept. of Chem. Engineering, Sweden.

Picado, A., & Gamero, R. (2014). Simulation of a continuous plug-flow fluidised bed dryer for rough rice. *Nexo*, 27(2), 115-124. doi: 10.5377/nexo.v27i2.1947

Picado, A., & Martínez, J. (2012). Mathematical modeling of a continuous vibrating fluidized bed dryer for grain. *Drying Technology*, 30(13), 1469-1481. doi: 10.1080/07373937.2012.690123

Pfost, H.B., Mourer, S.G., Chung, D.S., & Miliken, G.A. (1976). Summarizing and reporting equilibrium moisture data for grains (ASAE Paper No. 76-3520). St Joseph, MI: American Society of Agricultural Engineers.

Saravacos, G.D., & Maroulis, Z.B. (2001). Transport Properties of Foods. CRC Press. Boca Raton, USA. doi: 10.1201/9781482271010

Sun, D.W. (1998). Selection of EMC/ERH isotherm equations for shelled corn based on fitting to available data. *Drying Technology*, 16(3-5), 779-797. doi: 10.1080/07373939808917435

Wanjari, A.N., Thorat, B.N., Baker, C.G.J., & Mujumdar, A.S. (2006). Design and modeling of plug flow fluid bed dryers. *Drying Technology*, 24(2), 147-157. doi: 10.1080/07373930600558946

Yang, W.C. (2003). Handbook of Fluidization and Fluid-Particle Systems. CRC press. Boca Raton, USA. doi: 10.1201/9780203912744

Zoghi, T., Shahhoseini, S., Nosrati, K. (2018). New design of cross-flow fluidized bed dryers. *Amirkabir Journal of Mechanical Engineering*, 50(6), 1351-1360. doi: 10.22060/mej.2017.12564.5367